Ecological Indicators 125 (2021) 107474

Contents lists available at ScienceDirect

Ecological Indicators

journal homepage: www.elsevier.com/locate/ecolind

# The contributions of an airport and related road network to *Pseudevernia furfuracea* bioaccumulation of trace elements and polycyclic aromatic hydrocarbons

L. Lucadamo *, L. Gallo, G. Vespasiano, A. Corapi

*DiBEST (Department of Biology, Ecology and Earth Sciences), University of Calabria, 87036 Arcavacata di Rende, CS, Italy*

ARTICLE INFO

*Keywords:*
Airport
Road traffic
Trace elements
PAHs
Wind quantitative relationships
Particle diameter

ABSTRACT

The use of a high-density lichen transplant network together with quantitative wind relationships (WQRs) made it possible to evaluate the influence of an airport and surrounding road network on the spatial variation of polycyclic aromatic hydrocarbons (PAHs) and trace elements at both the local and whole study area scale. WQRs clearly showed that the parking/idling/taxiing area (PIT), but not the landing/take-off zones (LTZs), as well as the north/north-east part of the road network were contributors at the whole study area scale to the spatial variation of elements like Ni, Mo and V, i.e. those associated with ultrafine particles due to their involvement in anti-wear materials, and of total PAHs. In the case of an airport, such a result can have strong management implications. Traffic also affected the concentration of the prevailing volatile organic compounds. In contrast, LTZs and high traffic density values were correlated with peaks of Zn, Mo, Cu, Co, Mn, Ni, V, Al and Sb when associated with coarse particulate matter generated by deterioration of the landing gear, fuselage, wings, runway asphalt and brakes. The remarkable percentage of high-speed winds strongly affected both the spatial distribution of anthropogenic emissions and their atmospheric dilution, resulting in a rather low level of contamination. Our results suggest that biomonitoring can be much improved when matched with WQRs and that, in the event of high wind speeds, PAHs associated with the gas phase and fine/ultrafine particles are effective contamination tracers mainly at the whole study area scale whereas trace elements reveal contamination patterns at both scales.

## 1. Introduction

Adequate environmental management of atmospheric pollution at the mesoscale level requires the detection of potential anthropogenic sources of air contaminants. However, several approaches are possible considering the fundamental role of advection processes in affecting the spatial variation of elements and substances. Effective strategies should rely on the evaluation of quantitative relationships between the contaminant concentrations and air flows (Brusseau, 2006). Despite the opportunity provided by this kind of approach, in most literature reports, anemometric parameters were used merely to match trends in meteorological data with both particulate matter (PM) and Air Quality Index (AQI) variations, often with contrasting results. Indeed, while AQI shows a negative correlation with wind speed (Zhan et al., 2018; Liu et al., 2017), PM can have a negative or positive association depending on the size of the particulate matter (Wang et al., 2019), the exceeding of a specific wind speed threshold (Liu et al., 2017; Wang et al., 2019; Air Quality Expert Group, 2012) and the rising levels of $PM_{2.5}$ concentrations (Lv et al., 2017). Wind speed and direction are frequently used to predict pollutant dispersion models (Anu et al., 2015; Gunatilake et al., 2014), as well as to estimate the contribution to contamination of linear anthropogenic sources (Kim et al., 2015) or point sources, together with wind direction and distance of monitoring sites from a power utility (Riga-Karandinos and Karandinos, 1998).

Airports and related road traffic are typical anthropogenic sources of atmospheric pollutants whose environmental effect can be effectively studied by means of a quantitative approach to wind data. Given the role of several factors (climate, topography, size of the airport and related aircraft fleet, development of ground transportation routes, proximity to urban/city areas), road traffic and aviation compete for an overriding role in contaminant emissions. Aviation can contribute to atmospheric contamination both directly with emissions associated with the landing/

* Corresponding author.
*E-mail address:* lucio.lucadamo@unical.it (L. Lucadamo).

https://doi.org/10.1016/j.ecolind.2021.107474
Received 10 April 2020; Received in revised form 6 October 2020; Accepted 25 January 2021
Available online 15 February 2021

take-off (LTO) cycle and auxiliary power units (APUs) and indirectly due to ground support equipment (GSE) (Masiol and Harrison, 2014). Analyses of vehicle fuel efficiency have shown that the BTU/passenger mile (where BTU means the amount of energy needed to transport one passenger) decreased by 24% for aircraft between 2004 and 2012 while in the same period cars showed a reduction of only 8.8%, resulting in a higher final value (FAA, 2015).

On average, road transport is a stronger contributor of NOx and CO than airports, while the relative atmospheric input of total PAHs and PM seems to be comparable to ultrafine particles, sometimes being very intensely emitted by airport activities (Press-Kristensen, 2012; D'Agosto and Ribeiro, 2003; Choi et al., 2013). Many studies have evaluated potential toxic effects of airports on in situ workers and people residing in the surrounding area. In fact, exposure to diesel PM, 1–3 butadiene, benzene and acrolein was found to affect human health risks (Wood et al., 2008). Gaseous emissions, particularly CO, seem to be related to asthma and respiratory and heart problems, especially when excess idling takes place due to flight delays (Schlenker and Walker, 2016), while other evidence associates PM with the risk of cancer (Zhou and Levy, 2009).

Very few studies have used biomonitoring to assess the contribution of airports to environmental contamination. In one study, a local population of *Pinus eldarica* was used to evaluate the distribution of heavy metals, of which Cd and Zn showed the highest concentration at the sampling point close to Yazd Airport (Iran) (Miri et al., 2017). In another specific study on an airport (Nikola Tesla, Belgrade) using biomonitoring by means of moss bags located at four sites (runway, auxiliary runway and parking lot), Zn, Na, Cr, V, Cu and Fe showed the highest accumulation values (Vukovic et al., 2017). When concentrations of PAHs, heavy metals and trace metals were measured in curly kale and grass surrounding the Berlin Brandenburg Airport, all of them were comparable to or below the applicable maximum threshold (Waeber et al., 2015).

The present study is the first in which a wind quantitative parameter computed using wind speed and directions, the distances of sites from local contamination sources and periodic anemometric and contaminant monitoring were used in association with the epiphytic lichen transplantation technique to evaluate the contribution of a medium-size airport and surrounding road traffic to the atmospheric concentrations of trace elements and PAHs. The specific aims were to evaluate: a) the distribution of the contaminants, along with spatial patterns within the study area, b) the association, at the local scale (hundreds of squared meters from the potential source), between variation of the different zones of airport/traffic rate and those of trace elements and PAHs, and c) the potential role of airport and road transportation as sources, at the whole study area scale (tens of squared kilometres from the potential source), of trace elements and PAHs.

## 2. Materials and methods

### 2.1. Study area

The airport is situated in the municipality of Lamezia Terme (Calabria Region) and is one of the most important in southern Italy for passenger traffic (2,539,233) with a total aircraft movement of 17,302 per year (ENAC, 2017). It extends over 260 ha with two runways: an auxiliary one close to the apron area, devoted to parking and taxiing, and another where the LTO cycle takes place with a west-east orientation (Sacal, 2015). Airplanes usually land on the sea side of the runway and take-off from the land side (ENAC-ASSAEROPORTI, 2019). Three main roads cross the study area: SS18–Tirrenica Inferiore and Highway A2–del Mediterraneo from north to south, and SS280–dei Due Mari from north-east to north-west. In total, 55,915 vehicles circulate in the municipality of Lamezia Terme, corresponding to 613 per 1000 inhabitants, a datum closely approaching the national average (625) (ACI, 2016). Soils destined to agricultural use are mainly located on the south side of the monitored district, with arable land (22.5%) prevailing over arboriculture (16.3%) and vineyards (2.2%).

### 2.2. Lichen transplantation

Biomonitoring was performed by transplanting thalli of the epiphytic lichen *Pseudevernia furfuracea* from the Sila National Park to 40 sites selected in the study area, of which 14 (S5, S10, S14, S15, S16, S17, S21, S22, S24, S25, S26, S27, S29, S33) were considered suitable for monitoring airport activities because they were located inside it or near it (Fig. 1). In particular, 5 of them (S10, S14, S15, S16, S17) were positioned to evaluate the contribution of the parking/idling/taxiing area (PIT) activities to the atmospheric composition and 9 of them to evaluate the LTO cycle contribution. Such a partition of sites was set up because the airplanes stay for a longer time in the PIT zone than in the other parts, so that more than 1/3 of them were located there. The final density was 1.74 sites per square kilometre (within an area of 23 $km^2$), a rather high value that allowed a careful evaluation of the spatial variation of PAHs and trace elements. Lichen thalli were transplanted with their phorophytes and at each site were attached, with plastic strings, at a height of ca. 3 m above ground to minimize bias due to soil dust resuspension. The exposure lasted three months from 20 February to 20 May 2016. The mean yearly temperature, rainfall and relative humidity were respectively 17 °C, 890 mm and 74% in the study area and 10.1 °C, 1644 mm and 76.8% in the lichen origin area.

### 2.3. Contaminants analysis

#### 2.3.1. Trace elements

The elemental determination in the study area was performed on three subsamples for each of the 40 monitoring sites, while five subsamples were used for the lichen origin area. Thalli were immersed in liquid nitrogen until brittle, ground with a mortar and ceramic pestle and then mineralised with 12 mL of ultrapure nitric acid in a microwave oven (Milestone Ethos 900). The concentrations of Al, Mn, Ti, Ba, Cu, Zn, V, Cr, Co, Ni, As, Mo, Cd, Pb, Sb and Sn were measured by inductively coupled plasma-mass spectrometry (Elan DRC Perkin Elmer SCIEX) in the Mass Spectroscopy Laboratory of the Department of Biology, Ecology and Earth Sciences (University of Calabria). The accuracy and precision of the analysis were checked by means of the certified reference material BCR 482 (Lichen *Pseudevernia furfuracea* (L.) Zopf).

#### 2.3.2. Polycyclic aromatic hydrocarbons

The PAHs analysis was performed at Ecocontrol srl, Caraffa di Catanzaro (CZ). Five grams of dried thalli were first sonicated in 25 mL of acetone supplemented with 1 mL of internal standard (10 μg/mL) and then extracted with 25 mL of hexane. Following decantation, acetone was removed by means of mechanical stirring with double-distilled water and the use of a separating funnel. Due to the high clearness of samples, no silica gel filtration was needed. The extract was concentrated to 2 mL in a rotary vaporizer, dried (following the addition of toluene) under nitrogen flow and dissolved with 1 mL of internal standard for gas chromatography–mass spectrometry determination. The analysis was performed with a gas chromatograph equipped with an injection system in split/splitless modality and mass spectrometric detector. The column was a Zebron ZB-5MS plus. Run parameters were: 2 μL sample, flow of 1 mL/min, analyte quantification in single ion monitoring. Thirteen PAHs were searched for in thalli at the end of the exposure period: naphthalene; acenaphthene, phenanthrene, anthracene, fluoranthene, pyrene, benzo(a)anthracene, chrysene, benzo(b) fluoranthene, benzo(k)fluoranthene, benzo(a)pyrene, benzo(g,h,i)perylene, indeno(1,2,3-cd)pyrene.

### 2.4. Statistical analysis

Spatial patterns of trace elements and PAHs were evaluated by

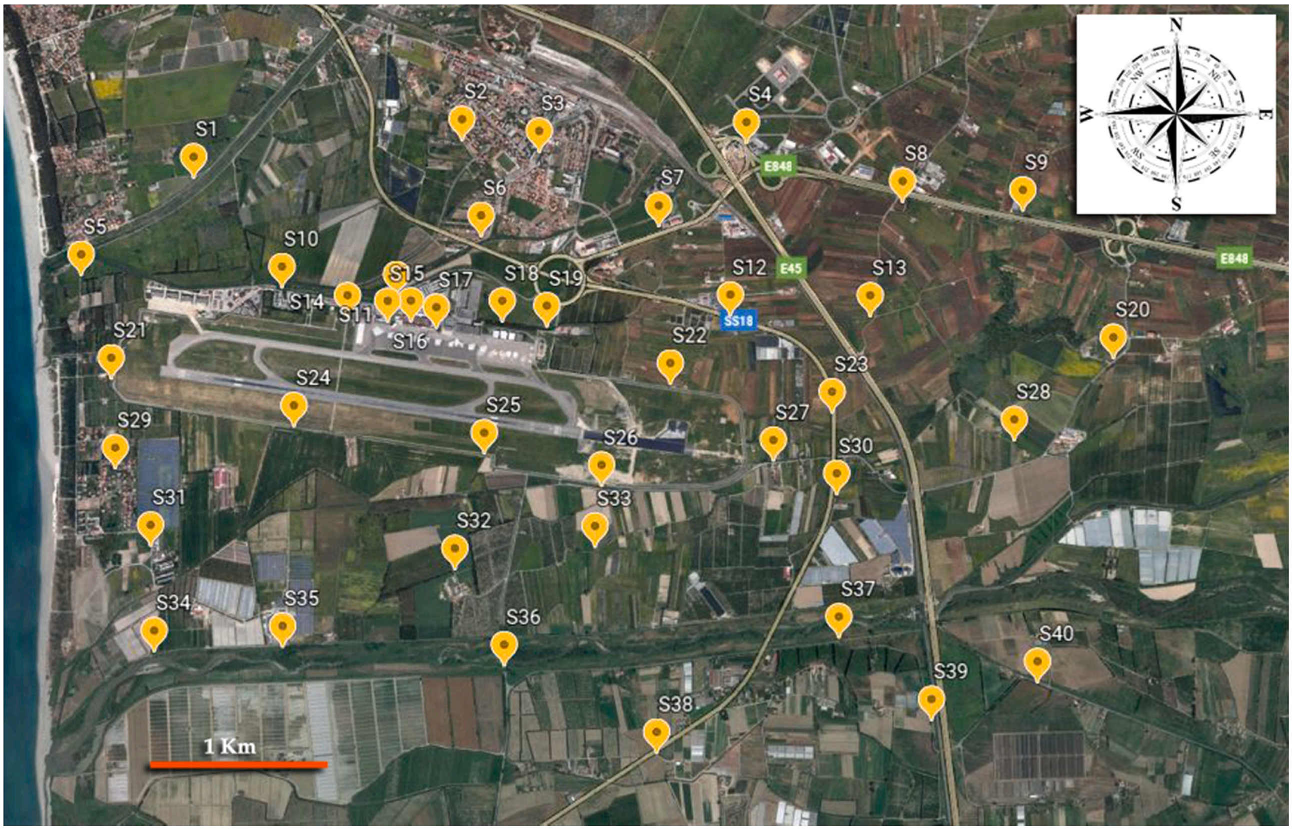


**Fig. 1.** Study area (figure taken from Google Earth and edited by the authors) showing the Lamezia Terme Airport, the main communication roads and the 40 sites where thalli were transplanted for biomonitoring activities.

means of a Detrended Correspondence Analysis (DCA) of the dataset: sites × potential contaminant ranks (polycyclic aromatic hydrocarbons and trace elements). Ranks were preferred to raw data to avoid clustering of macro- and microelements that could remove contamination trends.

To test the consistency of formed clusters, a Multi Response Permutation Procedure was performed using the factor "Groups". Kruskal-Wallis with Dunn test and Mann-Whitney test were used to test the null hypotheses: a) no difference between each cluster and the lichen origin area, b) no difference between the whole study area and the lichen origin area. The contribution at the local scale of the airport and road traffic to selected metals and organic compounds was evaluated by calculation respectively of the mean number of peaks (values within the 4th quartile range) of the PIT and LTO cycle zones and the correlation coefficient (Spearman) between the spatial variation of traffic rate and that of trace elements and PAHs.

The role of airport activities (idling, parking, taxiing, landing and take-off) and road traffic (number of cars, buses and trucks $h^{-1}$) as sources of atmospheric constituents at the whole study area scale was assessed by means of quantitative relationships with the wind, as explained below. Meteorological data (wind velocity, frequency and direction) were provided by the airport station of the Air Force meteorological service. These data were used, together with the distance of each site from all the others and the total exposure time of thalli, to calculate the parameter: Potential Number of Times Wind (passing through the zone where a hypothetical point source is located) Reaches the Sites (PNTWRS) in each geographical sector into which the study area is divided. This parameter has been successfully used by the authors to assess the contribution of point/diffuse sources of atmospheric contaminants (Lucadamo et al., 2016, 2017, 2018). It is the ratio between two times: the time wind flows in to each of the geographical sectors (as percentage of the transplant exposure time) and the time wind, passing through a potential point source, takes to reach sites located in each of the geographical sectors (in this case 8: NE, EN, ES, SE, SW, WS, WN, NW). This last value is calculated by dividing the distance separating the potential source from a site by the speed the wind flows into the geographical sector where the site is located. Each time a site is selected as a potential source it becomes the centrepiece of the wind rose with different sites attributed to the geographical sectors (see detailed example of calculation of PNTWRS, S1 in supplementary material).

This parameter can be easily calculated by means of a spreadsheet such as Excel. The rationale behind it is that the more the wind passing through a polluting source reaches a site where transplants are exposed the more there is a potential increase in pollutant bioaccumulation. Once the PNTWRS was computed, the role of sources at the whole study area scale was assessed as follows: 1) testing the significance of correlation coefficients (Spearman) related to the spatial variation of trace elements/PAHs and that of PNTWRS calculated for each site of the PIT and LTO cycle zones, referred to respectively as $R_{(PNTWRS\text{-}TE)}$ and $R_{(PNTWRS\text{-}PAHs)}$; 2) a two-step procedure of correlation coefficients (Spearman) determination: a) again testing the significance of the association between the spatial variation of trace elements/PAHs and PNTWRS ($R_{(PNTWRS\text{-}TE)}$ and $R_{(PNTWRS\text{-}PAHs)}$) calculated for each site considered not suitable to evaluate a local scale effect of the airport, b) evaluation of the statistical significance of the association, for each of the selected trace elements and PAHs, between the spatial variation of road traffic and that of the relative series of $R_{(PNTWRS\text{-}TE)}$ and $R_{(PNTWRS\text{-}PAHs)}$ of the above-mentioned type of sites. This second correlation, if successfully validated, would suggest that the more the traffic rate per site increases the more the contaminating role of that site at the level of the whole study area increases. The method of spatial interpolation (Inverse Distance Weighting (IDW)), often used in the Geographical Information System, has been applied for the generation of iso-concentration maps. The IDW method estimates values of cells by the weighting of values (points) of geometric data in the proximity of each processed area (cell). The points closer to the cell centre have more weight in the process of weighting. Multivariate analyses and uni/bivariate analyses were performed using the software PC-ORD 4 and Minitab 16 respectively.

## 3. Results

Anemometric results are shown in Table 1. Winds blow prevailingly from the west (49.6%) and least from the south (16.6%). Mean velocity is 2.4 $ms^{-1}$, with about 30% of winds showing a velocity higher than 5.5 $ms^{-1}$. However, when the high-speed series is considered, 58% of values are higher than 5.5 $ms^{-1}$ and 32% range from 8 to 23 $ms^{-1}$, suggesting that the area is characterized by a significant component of “dispersive” winds, i.e. diluting potential pollutants emitted by local sources.

Phenanthrene, fluoranthene, pyrene and chrysene are the only PAHs systematically detected at all sites, while anthracene and benzo(g,h,i) perylene show concentrations above the detection limit only at one site. About 64% of the trace element concentrations indicate absence of enrichment (Cr, As and Cd 100% of cases), 30% slight enrichment and only 6% moderate to high enrichment.

Fig. 2 shows the results of the Detrended Correspondence Analysis of the dataset sites × contaminants (PAHs and trace elements). Only the results of the first two axes are shown because most of the variance (62.7%) is associated with them. Based on the correlation between the ordination distances and distances in the original space (using relative Euclidean distance), two gradients are detectable, one along axis 1 (25.5% of variance) which separates cluster 2 from cluster 3 and a second one along axis 2 (37.2% of variance) which divides cluster 2 and 3 from cluster 1.

Application of a Multi Response Permutation Procedure, using the factor “Clusters” (i.e. the clusters resulting from DCA), supported the segregation between the detected groups ($T = -12{,}199$ $p = 0.000000$, chance-corrected within group agreement = 0.142). Sites of cluster 3 are mostly located in the north part of the study area (85% of sites), those of cluster 1 have an opposite distribution (100% in the south part), while sites of cluster 2 are more or less equally distributed between the two parts (42% north, 58% south). The highest concentrations of the most representative PAHs (total PAHs included) are found at sites of cluster 3 (Table S1). Cluster 2 does not differ from cluster 3 only in the case of pyrene, while it always shows higher concentrations than cluster 1.

As regards the trace elements (Al, V, Cr, Cu, Ni, As, Mo, Pb, Ti, Sn, Sb, Ba), the highest concentrations were detected at sites of cluster 2 followed by those of cluster 3, with the lowest ones measured in cluster 1 (Table S2). Both trends were supported by the results of a 1-way non-parametric ANOVA and Dunn test (Tables S3, S4). When the mean concentrations of the elements are considered at the level of the whole study area, all of them show a marked (Mann-Whitney $p < 0.05$) difference from the LOA, except Mn, Mo and Cd.

The analysis of the local scale effects of the investigated pressures, i.e. when evaluated respectively at the sites within/very close to Lamezia Terme Airport and at those located in the remaining part of the study area (chosen to monitor road traffic), reveals peculiar spatial trends. Values of Al, V, Co, Ni, Cu, Zn, Mo, Ti, Sb and Sn related to the 4th quartile were detected at several sites of the airport. However, when the different zones are considered, an asymmetric distribution is evident. Indeed, the mean number of peaks per site (MPS) is the following: sea side (landing) of runway = 4.3, land side (take-off) = 4.0 and PIT zone = 1.0. In contrast, the MPS is quite low for PAHs. In fact, the number of concentrations related to the 4th quartile of phenanthrene, fluoranthene, chrysene, pyrene and total PAHs shows the following pattern: sea side of runway = 1.0, land side = 1.2 and PIT = 1.0 (peaks only at site S17). The non-parametric correlation analysis (Spearman) between the spatial variation of traffic rate (vehicles $h^{-1}$) and that of the investigated substances shows a significant coefficient for Cu, Mo and Sb, measured separately for cars (Mo: $r = 0.364$, $p = 0.029$; Sb: $r = 0.354$, $p = 0.034$) and trucks/buses (Cu: $r = 0.332$, $p = 0.048$; Mo: $r = 0.503$, $p = 0.002$; Sb: $r = 0.410$, $p = 0.013$). No significant correlations were detected for PAHs. The airport and vehicle circulation are also effective sources of trace elements and PAHs at the whole study area scale (kilometres from the source). Table 2 shows the statistically significant correlations between the PNTWRS calculated for the sites chosen to monitor airport emissions and the spatial variation of trace elements.

All five sites related to the PIT zone (S10, S14, S15, S16, S17) show significant coefficients (16 of the total 19) respectively with Co, Cu, Mn, Mo, Ni, V and Zn, while the PNTWRS of only 2 (S5 and S21) of the 9 sites located in/near the landing/take-off zones are significantly correlated with the spatial variation of Mn and Mo (3 of the 19 coefficients). Table 3 lists these correlations with PAHs, and only the PNTWRS of the five sites (S10, S14, S15, S6, S17) monitoring the PIT zone are significantly correlated with the spatial variation of total PAHs.

Tables 4 and 5 show the results (significant coefficients) of the correlation analysis between the PNTWRS calculated for each of the sites not specifically monitoring airport activities (i.e. the 26 sites located outside the airport and monitoring the traffic circulation) and the spatial variation of respectively the trace elements and the PAHs.

As at the airport monitoring sites, the elements with the highest number of significant correlations were Mo, Ni and V with the addition of Cu. Phenanthrene, fluoranthene, pyrene and total PAHs always showed significant coefficients for the same group of sites except S13 (Table 5). Interestingly, positive correlations were systematically found, for both trace elements and PAHs, exclusively at sites north of the airport whereas negative correlations were found only at sites south of the airport.

Once the coefficients $PNTWRS_{-TE}$ and $PNTWRS_{-PAHs}$ were calculated, their spatial variation was correlated (Spearman) with the spatial variation of traffic rate. The rationale of this correlation is that the more the traffic circulation increases at a site the more that site is a point source of a trace element or a PAH. The new coefficients were calculated separately for type of vehicles, and the statistically significant ones are the following: **Cars**: Co, $r = 0.46$, $p = 0.004$; Mn, $r = 0.504$, $p = 0.002$; Mo, $r = 0.47$, $p = 0.004$; Ni, $r = 0.56$, $p < 0.0005$; V, $r = 0.432$, $p = 0.008$; P, $r = 0.49$, $p = 0.002$; Fl, $r = 0.52$, $p = 0.001$; Py, $r = 0.50$, $p = 0.002$; Chr, $r = 0.50$, $p = 0.002$; total PAHs, $r = 0.513$, $p = 0.001$; **Trucks/Buses**: Mo, $r = 0.398$, $p = 0.016$; V, $r = 0.357$, $p = 0.033$; P, $r = 0.40$, $p = 0.016$; Fl, $r = 0.38$, $p = 0.024$; Py, $r = 0.41$, $p = 0.013$; Chr, $r = 0.43$, $p = 0.010$; total PAHs, $r = 0.518$, $p = 0.001$.

Figs. 3–6 show the isoconcentration maps of Mo, V, Ni and total PAHs, i.e. those substances whose spatial variation was mostly affected by the role as sources, at the whole study area level, of PIT sites and those sites not dedicated to airport monitoring and located in the north-north-east zone, where the highest values of traffic rate were measured.

**Table 1**
Mean values of wind frequency and velocity based on daily records. The frequency of data recording was set once every 15 min for a total of 8300 records at the end of the transplant exposure (three months). Daily velocity was calculated as the mean of the 96 records. Daily frequency was expressed as the percentage of the 96 records. High speed: the highest velocity recorded every 15 min.

| | N | NE | E | SE | S | SW | W | NW |
|---|---|---|---|---|---|---|---|---|
| Frequency (%) | 0.05 | 16.88 | 24.57 | 3.31 | 5.61 | 7.65 | 34.66 | 7.27 |
| Velocity (m $s^{-1}$) | 1.73 | 3.57 | 3.80 | 0.49 | 1.05 | 2.20 | 5.25 | 5.19 |
| Highspeed (m $s^{-1}$) | 2.53 | 5.98 | 7.05 | 2.79 | 3.35 | 5.28 | 7.61 | 7.43 |

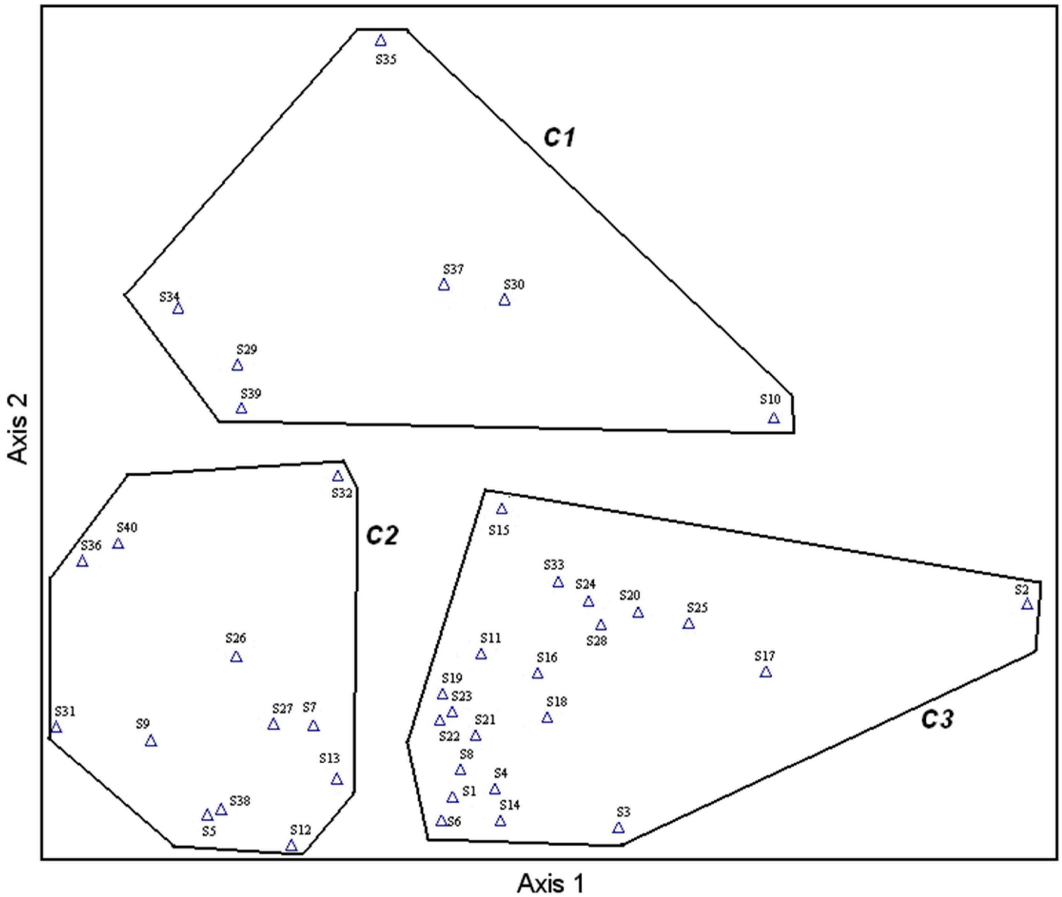


**Fig. 2.** Ordination diagram resulting from a Detrended Correspondence Analysis (number of segments: 26) of the dataset sites × contaminants (polycyclic aromatic hydrocarbons and trace elements). Only the ordination relative to the first two axes is shown because they explain most of the variance (62.7%). Three clusters are detectable: C1, C2, C3.

**Table 2**
Testing the potential role as "point source" of the 14 sites (see Section 2.2 paragraph) selected to monitor the two different airport zones (LTO zone and PIT zone). This means calculating the Potential Number of Times that Wind, passing through each of these 14 sites, Reaches the remaining 39 Sites (PNTWRS). The table shows only the statistically significant non-parametric correlation coefficients (r) (Spearman) between the spatial variation of PNTWRS and the spatial variation of the thalli concentrations of selected trace elements (μg/g d.w. of lichen thallus) measured at 39 of 40 sites (the site tested for its role as point source is obviously excluded). p = levels of probability, S = site.

| SITES | Co | | Cu | | Mn | | Mo | | Ni | | V | | Zn | |
|---|---|---|---|---|---|---|---|---|---|---|---|---|---|---|
| | r | p | r | p | r | p | r | p | r | p | r | p | r | p |
| S5 | – | – | – | – | 0.35 | 0.031 | 0.34 | 0.032 | – | – | – | – | – | – |
| S10 | 0.35 | 0.03 | – | – | 0.51 | 0.001 | 0.32 | 0.045 | 0.52 | 0.001 | 0.38 | 0.018 | – | – |
| S14 | – | – | – | – | – | – | 0.47 | 0.002 | 0.37 | 0.02 | – | – | – | – |
| S15 | – | – | – | – | – | – | 0.41 | 0.009 | 0.32 | 0.049 | 0.34 | 0.035 | – | – |
| S16 | – | – | – | – | – | – | 0.36 | 0.025 | – | – | – | – | – | – |
| S17 | 0.36 | 0.023 | 0.46 | 0.003 | – | – | – | – | 0.37 | 0.021 | 0.32 | 0.045 | 0.34 | 0.035 |
| S21 | – | – | – | – | – | – | 0.46 | 0.003 | – | – | – | – | – | – |

Peak partition is well evident, within the airport, in the case of Ni and V and less evident for Mo. Both trace elements and PAHs show, on average, higher concentrations in thalli mainly in the northern part of the study area and lower values in the southern one.

## 4. Discussion

### *4.1. Distribution of the monitored substances and their spatial patterns*

The results of the three months of biomonitoring using *Pseudevernia furfuracea* transplantation suggest the development of a different spatial pattern for PAHs and trace elements. The former show the highest values of bioaccumulation in the north part of the study area consistently with the location of their main anthropogenic sources (airport and road network). The only PAHs systematically detected at all sites were phenanthrene, fluoranthene, pyrene and chrysene. These are 3–4 ring compounds present in gas (P) and gas/particulate phases (Fl, Py, Chr) (Bostrom et al., 2002). In exhaust from both gasoline/petrol and diesel fuelled vehicles, the gas-particulate ratio of these compounds amounts, on average, to 50% (Benner et al., 1989; Ho et al., 2009), depending on the levels of engine maintenance and the presence of catalytic equipment, with particles ranging from fine to ultrafine size (Hall et al., 1998a). Studies of aircraft emissions show that these same PAHs are typically found in gaseous exhausts with a gas/particulate partition ratio

**Table 3**
Testing the potential role as "point source" of the 14 sites (see Section 2.2) selected to monitor the two different airport zones (LTO zone and PIT zone). This means calculating the Potential Number of Times that Wind, passing through each of these 14 sites, Reaches the remaining 39 Sites (PNTWRS). The table shows only the statistically significant non-parametric (Spearman) correlation coefficients (r) between the spatial variation of PNTWRS and the spatial variation of the thalli concentrations of the detected polycyclic aromatic hydrocarbons (μg/g d.w. of lichen thallus) measured at 39 of 40 sites (the site tested for its role as point source is obviously excluded). p = levels of probability, S = site.

| SITES | Phenanthrene | | Fluoranthene | | Pyrene | | Total PAHs | |
|---|---|---|---|---|---|---|---|---|
| | p | r | p | r | p | r | p | r |
| S5 | 0.49 | 0.002 | 0.47 | 0.005 | 0.48 | 0.002 | – | – |
| S10 | – | – | – | – | – | – | 0.33 | 0.039 |
| S14 | – | – | – | – | – | – | 0.43 | 0.006 |
| S15 | 0.32 | 0.048 | 0.36 | 0.025 | 0.33 | 0.043 | 0.39 | 0.016 |
| S16 | 0.038 | 0.017 | 0.35 | 0.029 | – | – | 0.37 | 0.022 |
| S17 | 0.036 | 0.024 | – | – | – | – | 0.36 | 0.021 |
| S21 | 0.39 | 0.014 | 0.34 | 0.036 | – | – | – | – |

presenting a wide range, with a median of 9.6 (Kuhlman and Chuang, 1989). The other polycyclic aromatic hydrocarbons, scarce in the lichen transplants, have higher molecular weights (5 and 6 rings) and, when emitted, are usually bound to particulate matter. Previous monitoring activities to investigate the road traffic contribution to the atmosphere utilizing lichens, with the same species used by the present authors (Guidotti et al., 2009) and a different one (*Evernia prunastri*) (Blasco et al., 2008), gave similar results, with 2–4 ring PAHs being the most accumulated in thalli and heavier compounds accumulated much less. These results suggest that lichens not only effectively trap both gas and particulate phases of PAHs but also in a ratio that largely matches their emissions from anthropogenic sources (Keyte et al., 2016; Vieira de Souza and Correa, 2016).

The spatial pattern of trace elements is more complex, probably because their sources are distributed between the north and south parts of the study area. Indeed, in both of these parts (cluster 2), agriculture is quite intensely practised (viticulture, olive cultivation and arable land). Plowing of the land and the lack of cover grass in vineyards and olive groves can promote soil erosion, resulting in an increase of bioaccumulation of elements such as Al, Ti, and Ni and Co due to the presence of Vertisols in the study area (ESDAC, 2020; Serelis et al., 2010). Moreover, when sprayed, organotin and sodium arsenite based pesticides may contribute to the drift of As and Sn (EURL-SRM, 2013), although the former are used much less today than in the past (Songy et al., 2019). On the other hand, traffic and airport activity can be important environmental sources of elements such as Al, V, Co, Mo, Ni, Cu, Mo, As, Sn, Sb and Pb (Johansson et al., 2008; Pant and Harrison, 2013; Masiol and Harrison, 2014; TRANSPHORM, 2014), resulting in an additional contribution in the north part of the study area. Despite the presence of several potential sources of trace elements, the significant frequency of "dispersive" wind velocities reduced thalli bioaccumulation, so that no or very low levels of enrichment were detected compared to the pre-exposure amounts.

### 4.2. *Variation of the selected human pressures and that of trace elements and PAHs at the local scale*

In the airport, most of the trace elements showed a differential pattern of the mean number of peaks per site, with higher values in the landing (4.3) and take-off (4.0) sides of the airport runway and lower ones in the PIT zone (1.0). Many of them (Zn, Mo, Cu, Co, Mn, Ni, V, Al) can arise from wear of the runway asphalt (Bennett et al., 2011), deterioration of brakes and landing gear (Amato et al., 2010), fuselage and wing corrosion due to atmospheric agents, pollutants and de-icing substances sprinkled on the runway surface (Usmani and Donley, 2002; Huttunen-Saarivirta et al., 2011). All the particles resulting from these processes have a mean diameter of 1 to 10 μm (Danish EcoCouncil, 2019), i.e. they are considered "coarse particulate". In addition, these particles are affected by gravitational settling with a high deposition velocity (Mohan, 2016), suggesting that they are effective markers of related sources at the local scale. This result is consistent with the hypothesis that both the runway surface and mechanical components of aircraft suffer stronger physical–chemical stresses in the landing/take-off zones than in the PIT area. Other studies measuring metal levels in soils surrounding airports, and sometimes investigating landing/take-off paths, found an association between airport activities and several elements, including Cu, Ni, Co, V and Zn (Boyle, 1996; Nunes et al., 2011; Massas et al., 2016), thus partially supporting our findings.

When trace elements were evaluated as local-scale markers for

**Table 4**
Testing the potential role as "point source" of the sites not specifically monitoring the airport (i.e. the 26 sites located outside the airport, including those related to the large parking area in proximity to the layover). This means calculating the Potential Number of Times that Wind, passing through each of these 26 sites, Reaches the remaining 39 Sites (PNTWRS). The table shows only the statistically significant non-parametric (Spearman) correlation coefficients (r) between the spatial variation of PNTWRS and the spatial variation of the selected trace elements (μg/g d.w. of lichen thallus) measured at 39 of 40 sites (the site tested for its role as point source is obviously excluded). p = levels of probability, S = site. These correlations are denoted as $R_{(PNTWRS-TE)}$.

| North of Airport | Co | | Cu | | Mn | | Mo | | Ni | | Sb | | V | |
|---|---|---|---|---|---|---|---|---|---|---|---|---|---|---|
| | r | p | r | p | r | p | r | p | r | p | r | p | r | p |
| S1 | – | – | – | – | 0.53 | <0.0005 | 0.41 | 0.009 | 0.45 | 0.004 | – | – | – | – |
| S4 | – | – | – | – | – | – | 0.33 | 0.043 | 0.46 | 0.003 | – | – | – | – |
| S6 | – | – | – | – | – | – | 0.33 | 0.042 | 0.394 | 0.013 | – | – | – | – |
| S7 | – | – | – | – | – | – | 0.42 | 0.007 | 0.32 | 0.044 | – | – | – | – |
| S8 | 0.33 | 0.042 | 0.32 | 0.05 | – | – | 0.34 | 0.036 | 0.49 | 0.002 | 0.43 | 0.006 | 0.35 | 0.03 |
| S9 | – | – | 0.47 | 0.002 | – | – | 0.40 | 0.012 | – | – | – | – | 0.35 | 0.029 |
| S11 | – | – | 0.32 | 0.05 | 0.34 | 0.036 | 0.41 | 0.010 | – | – | – | – | – | – |
| S13 | – | – | 0.33 | 0.041 | – | – | 0.43 | 0.006 | 0.41 | 0.009 | – | – | 0.43 | 0.007 |
| S19 | – | – | – | – | – | – | 0.36 | 0.022 | – | – | – | – | – | – |
| South of Airport | r | p | r | p | r | p | r | p | r | p | r | p | r | p |
| S28 | −0.38 | 0.016 | – | – | – | – | – | – | – | – | – | – | – | – |
| S30 | – | – | – | – | −0.41 | 0.010 | – | – | – | – | – | – | – | – |
| S31 | – | – | – | – | – | – | – | – | −0.32 | 0.044 | – | – | – | – |
| S34 | −0.38 | 0.016 | −0.36 | 0.024 | −0.34 | 0.033 | – | – | −0.48 | 0.002 | – | – | −0.40 | 0.013 |
| S35 | – | – | – | – | – | – | −0.38 | 0.016 | – | – | – | – | – | – |
| S36 | – | – | – | – | −0.33 | 0.041 | – | – | −0.34 | 0.034 | – | – | – | – |
| S37 | – | – | – | – | – | – | −0.35 | 0.029 | – | – | – | – | – | – |
| S39 | – | – | – | – | −0.46 | 0.004 | – | – | – | – | – | – | – | – |
| S40 | – | – | −0.36 | 0.026 | – | – | −0.34 | 0.034 | – | – | – | – | – | – |

**Table 5**
Testing the potential role as "point source"of the sites not specifically monitoring the airport (i.e. the 26 sites located outside the airport, including those related to the large parking area in proximity to the layover). This means calculating the Potential Number of Times that Wind, passing through each of these 26 sites, Reaches the remaining 39 Sites (PNTWRS). The table shows only the statistically significant non-parametric (Spearman) correlation coefficients (r) between the spatial variation of PNTWRS and the spatial variation of detected polycyclic aromatic hydrocarbons (μg/g d.w. of lichen thallus) measured at 39 of 40 sites (the site tested for its role as point source is obviously excluded). p = levels of probability, S = site. These coefficients are denoted as $R_{(PNTWRS\text{-}PAHs)}$.

| North of airport | Phenanthrene | | Fluoranthene | | Pyrene | | Chrysene | | Total PAHs | |
|---|---|---|---|---|---|---|---|---|---|---|
| | r | p | r | p | r | p | r | p | r | p |
| S1 | 0.52 | 0.001 | 0.61 | <0.0005 | 0.60 | <0.0005 | 0.43 | 0.006 | 0.52 | 0.001 |
| S3 | 0.36 | 0.025 | 0.44 | 0.005 | 0.46 | 0.003 | – | – | 0.35 | 0.029 |
| S4 | 0.44 | 0.005 | 0.51 | 0.001 | 0.47 | 0.002 | – | – | 0.48 | 0.005 |
| S6 | 0.37 | 0.021 | 0.42 | 0.008 | 0.37 | 0.019 | – | – | 0.36 | 0.022 |
| S8 | 0.52 | 0.001 | 0.59 | <0.0005 | 0.64 | <0.0005 | 0.35 | 0.027 | 0.59 | <0.0005 |
| S9 | 0.55 | <0.0005 | 0.57 | <0.0005 | 0.54 | <0.0005 | 0.35 | 0.027 | 0.57 | <0.0005 |
| S11 | 0.43 | 0.006 | 0.43 | 0.006 | 0.41 | 0.009 | – | – | 0.46 | 0.003 |
| S13 | – | – | 0.36 | 0.026 | 0.33 | 0.040 | – | – | 0.42 | 0.008 |
| South of Airport | r | p | r | p | r | p | r | p | r | p |
| S31 | −0.322 | 0.045 | −0.49 | 0.002 | −0.52 | 0.001 | −0.35 | 0.03 | −0.45 | 0.009 |
| S34 | −0.36 | 0.024 | −0.43 | 0.006 | −0.40 | 0.012 | – | – | −0.35 | 0.03 |
| S36 | −0.38 | 0.017 | −0.40 | 0.011 | −0.32 | 0.048 | – | – | −0.39 | 0.014 |
| S37 | −0.41 | 0.01 | −0.48 | 0.002 | −0.44 | 0.005 | −0.41 | 0.009 | −0.42 | 0.007 |
| S39 | −0.51 | 0.001 | −0.54 | <0.0005 | −0.47 | 0.003 | −0.43 | 0.006 | −0.47 | 0.003 |

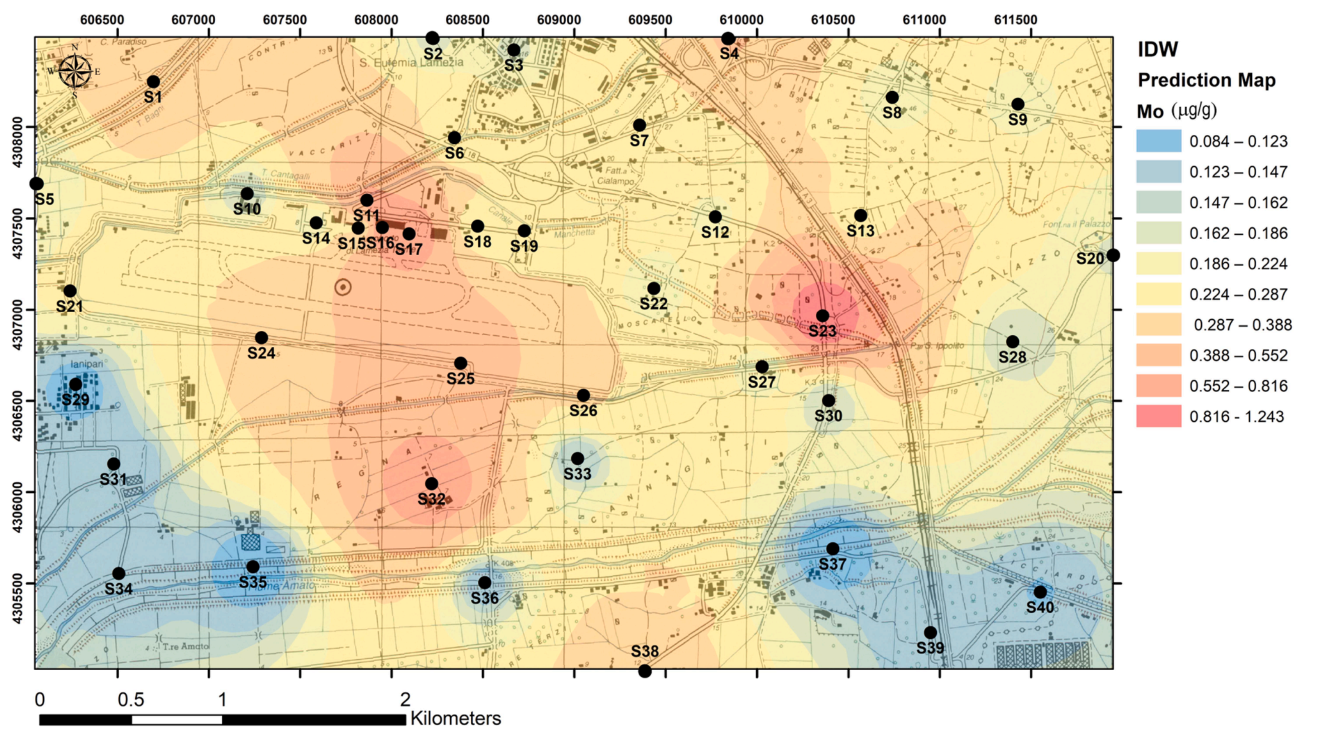


**Fig. 3.** Isoconcentration map of molybdenum.Inverse Distance Weighting (IDW) was used to generate the map. Different colours denote different concentration areas based on the scale shown on the right side of the figure (μg/g d.w. of lichen thallus).

variation in the road traffic rate, the results confirmed the above-mentioned interpretation of the effect of the size of particles the metals are linked to on their spatial distribution. Indeed, there were significant correlations between the number of vehicles $h^{-1}$ and thalli concentrations of Cu, Mo and Sb, the primary components of brake pads, whose wear results in the formation of dusts with a size mode ranging from 1.6 to 2 μm (Dongarrà et al., 2009) to 4 μm (Iijima et al., 2007), a type of coarse particulate with a significant deposition rate in the surroundings of the emission source. Only one site in the parking/idling/taxiing zone (S17) showed peaks of all the PAHs systematically detected in the study area, while sites on the landing/take-off runway sides showed a lower mean number of peaks (sea side = 1.0, land side = 1.2). Surprisingly, the spatial variation of traffic was never associated with that of PAHs. We believe that this result is due to the interaction among the gas/particulate phase ratio, the size of emitted particles and the intensity and frequency of high wind speeds. Further explanation will be given in the following section by comparison with the analysis of variation at the whole study area scale.

### *4.3. Evaluation of the role of airport and road traffic as sources of trace elements and PAHs at the whole study area scale*

This analysis was made possible by the use of a quantitative wind parameter (PNTWRS) that allowed testing of the potential role of a single monitoring site as a point source of selected substances at the level of the whole study area. This parameter is the potential frequency the

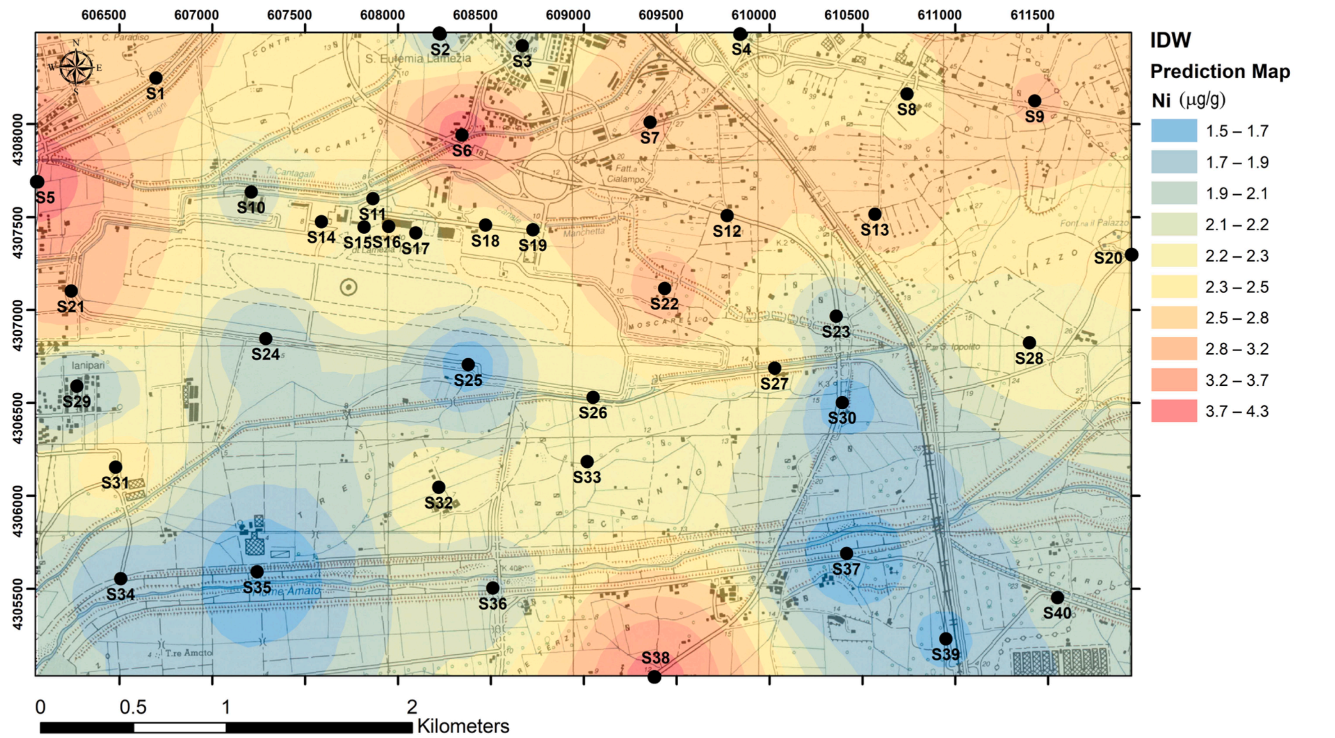


**Fig. 4.** Isoconcentration map of nickel. Inverse Distance Weighting (IDW) was used to generate the map. Different colours denote different concentration areas based on the scale shown on the right side of the figure (μg/g d.w. of lichen thallus).

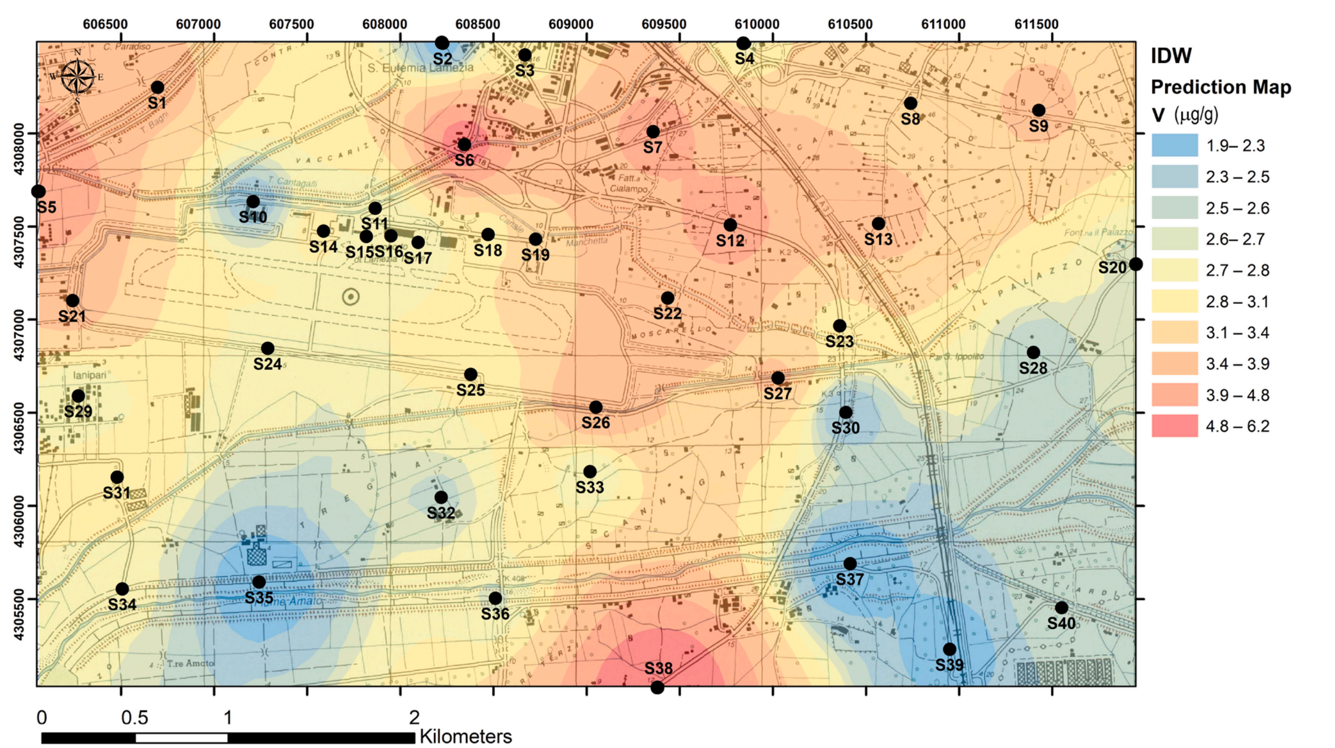


**Fig. 5.** Isoconcentration map of vanadium. Inverse Distance Weighting (IDW) was used to generate the map. Different colours denote different concentration areas based on the scale shown on the right side of the figure (μg/g d.w. of lichen thallus).

wind, passing through a "candidate" point source, reaches each of the sites located on each geographical side during the monitoring period (Lucadamo et al., 2016). Once calculated, it is correlated with the spatial variation of the substances of interest. In the case of trace elements, significant correlations were found mainly for Mo and Ni, and secondarily V, for both the airport and road traffic rate probably because they involve similar applications in terms of materials and anti-wear methodologies. Only sites in the airport's PIT zone can be considered potential sources of these elements at the whole study area scale (84% of all significant correlations vs 16% associated with landing/take-off sites,

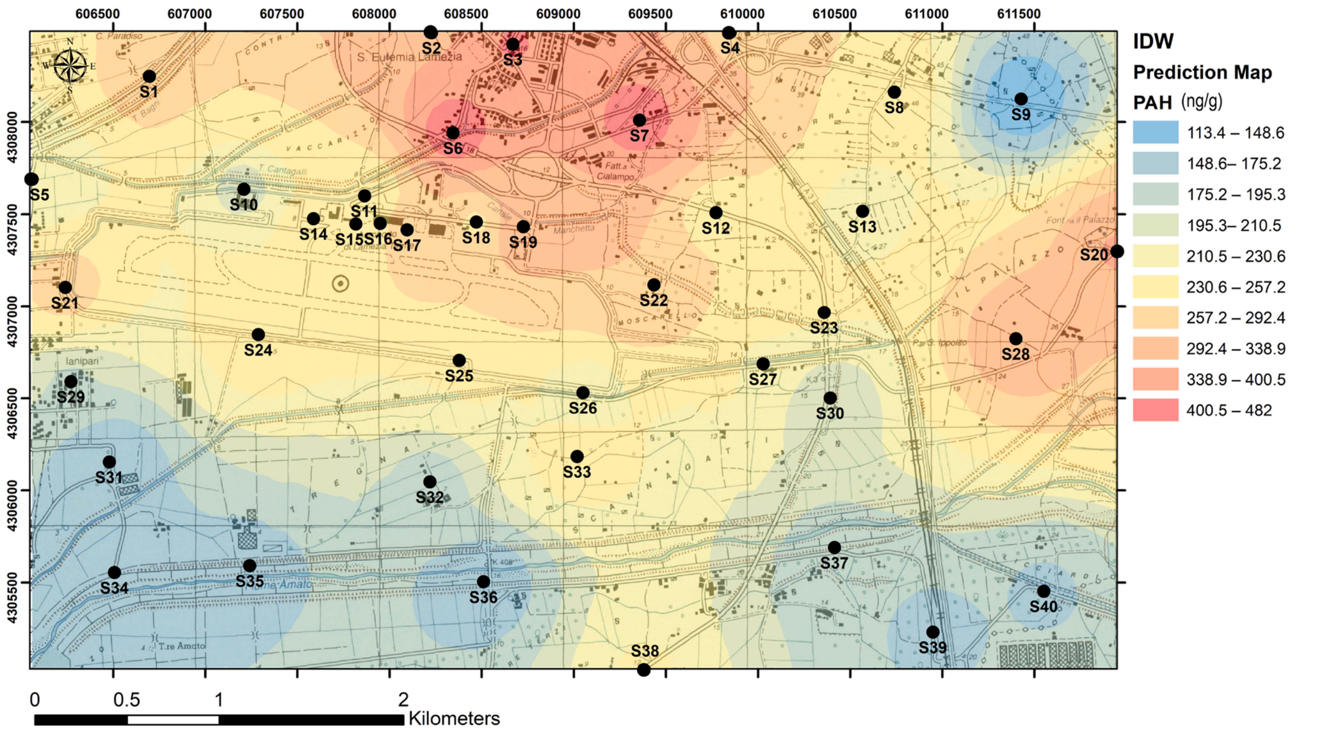


**Fig. 6.** Isoconcentration map of total PAHs. Inverse Distance Weighting (IDW) was used to generate the map. Different colours denote different concentration areas based on the scale shown on the right side of the figure (μg/g d.w. of lichen thallus).

Table 4), probably because the activities generating them are much longer-lasting in this part of the airport than in the rest of the airport. After landing, the aircraft engine is switched off and an auxiliary power unit (APU), i.e. a secondary engine, is switched on to support the airplane's functions. When the aircraft stops in the parking zone, the APU may or may not be switched off. The first option is called single cycle APU event. The second is called double cycle APU event, during which the airplane is connected to an external power unit (ground support equipment – GSE). These are usually powered by diesel engines which, on average, burn more than 7.5 kg of fuel per hour (Fleuti and Hofmann, 2005), emitting 6.3 tons of VOC per year (Kenney et al., 2015) and, potentially, the same range of trace elements associated with oil and lubricants of on-road vehicles (see below). They operate until the APU is switched on again before the airplane moves from the parking zone. The supplied power is needed to support the control panel, air conditioning and air bleeding of the engine. Unfortunately, APU reactivation often takes place long before the effective take-off time due to delays caused by various factors, resulting in higher aircraft fuel consumption and relative emissions. The whole turnaround lasts an average of 45 min (Padhra, 2018), ranging from 25 to 120 min, far longer than the periods the aircraft is involved in the landing and take-off phases. In the aerospace industry, Ni and Mo are used to manufacture alloys of the APU (Kracke, 2010) and they are also primary components of the Hastelloy X alloy of the main jet turbine, with the latter element often used in lubricant applications, while V is found in kerosene and oil (Abegglen, 2016). In addition, these three elements are typically associated with the soot emitted by jet engines, with molybdenum being a quite significant component at low thrust (Abegglen, 2016), as well as with the APU exhaust, being found as wear particles in oil samples (AZO Materials, 2009). Analysis of emitted particles from both types of power units show that their size mode ranges from 20 to 40 nm for the APU (Kinsey et al., 2012) and around 20 nm for the primary engine at the lowest power (idling). Such diameters classify them as "ultrafine" particles, i.e. affected by Brownian diffusion in their deposition trajectories so that they have a quite long suspension time (Sehmel and Hodgson, 1978; Fang et al., 1997).

This theoretical framework is consistent with our monitoring results. Sites S10, S14, S15, S16 and S17 (very close to or within the PIT zone) are those where the APU, GSE and main jet engine at lowest thrust operate for prolonged times, so that they become primary airport sources of these three elements at the level of the whole study area by means of winds often blowing at speeds that strongly disperse the emissions. Molybdenum, probably due to a higher emission rate (in soot at low thrust) than V and Ni, also shows some peaks at the local scale (sites S16 and S17). Road traffic is also a comparable and continuous source of these trace elements. Interestingly, molybdenum, as well as being used as a component of brake pads, is found as disulphide nanoparticles in additives of oil lubricants, i.e. the emitted particle size is expected to have a bimodal distribution, respectively around 2–4 μm and tens-hundreds of nanometres. V and Ni are similarly found in car oil lubricants and are associated with exhaust particles with a diameter ranging from 500 nm to 1 μm (Sarvi et al., 2011), a value that also results in very slow deposition velocities (Mohan, 2016). When the correlations, for each trace element, between the site-($R_{(PNTWRS\text{-}TE)}$) (Table 4) and that of the traffic rate were considered, Mo, Ni and V again showed significant coefficients together with Co and Mn. However, Mo, Ni and secondarily V showed the highest number of statistically significant site-($R_{(PNTWRS\text{-}TE)}$) (Table 4), suggesting that they are the most consistent tracers of long-range emissions for road traffic. In addition, all the positive site-($R_{(PNTWRS\text{-}TE)}$) were found in the north part of the study area, i.e. where there were the highest levels of traffic rate, whereas all the negative site-($R_{(PNTWRS\text{-}TE)}$) were found in the south part, with the lowest traffic rate levels. While a positive coefficient can be considered to support the potential role of a site as a point source of these metals, a negative coefficient can indicate a site substantially lacking sources of these elements, so that the more the wind passes through that site the more it helps to dilute the concentration of the metals at the remaining sites.

The lichen bioaccumulation pattern of PAHs seemed only relatively comparable to that of trace elements. The PIT monitoring sites showed a similar number of significant site-($R_{(PNTWRS\text{-}PAHs)}$) compared to the landing/take-off sites, although only the former (S10, S14, S15, S16, S17) can be considered sources of total PAHs at the whole study area scale (Table 3). Indeed, many literature reports clearly indicate that aircraft engines emit much higher PAH levels at minimum-low thrust than at higher power (EASA, 2013; Spicer et al., 1990; Kuhlman and Chuang, 1989; Agrawal et al., 2008). Moreover, considering the substantial contribution to emissions of volatile and semivolatile PAHs due to the long operating times of the APU and GSE (Zielinska et al., 2004) (like the primary engine when involved in prolonged taxiing; Zhang and Wang, 2017) as well as the prevalent association of PAHs with the gaseous phase and with nanoscale particles (Rogers et al., 2005) and the significant frequency of wind dispersive velocities, the activities taking place in the apron area (including taxiing to move toward the runway) effectively contributed to the spatial variation of both trace elements and PAHs at the level of the whole study area. Based on these considerations, we hypothesize that the relatively low number of peaks (4th quartile values) found within/very close to the airport may be due to the quick removal of the emissions by frequent strong winds that reduce bioaccumulation at the local scale. Analysis of the correlations, for each of the systematically detected PAHs, between the traffic rate and site-($R_{(PNTWRS\text{-}PAHs)}$) supports the role of road traffic in promoting emissions with long-range (several square kilometres) deposition. PAHs associated with exhausts of both diesel and gasoline/petrol fuelled car engines contain, in addition to a gaseous component, ultrafine particles with a size mode between 10 and 250 nm (Xue et al., 2015; Hall et al., 1998b; Szewczynska et al., 2017), which in our study area were emitted with a higher frequency in the north part (median 52 vehicles $h^{-1}$, min 2, max 1712) and were blown away by quite constant dispersive winds. This datum is of paramount importance because it matches that for the trace elements and further strengthens the conclusion that the emissions associated with the higher road traffic rate in the north side affected the spatial variation of both these substances at the level of the whole study area (23 $km^2$). Again, we believe that the lack of correlations between traffic rate and PAHs at the local scale was probably due to the significant frequency of high-speed winds that effectively removed the vehicle exhausts from the emission site, thus preventing an appreciable transplant bioaccumulation “in situ”.

The very small height of emission sources, 1.5–2 m (main turbines), 2–3 m (APU) and 30–60 cm (GSE/car tailpipe), did not prevent these anthropogenic activities from affecting the long-range distribution of emitted substances, suggesting that the wind velocity and frequency, as well as the gas/particulate partition and size of emitted particles, are the main factors determining the length of the deposition trajectories.

## 5. Conclusions

The results of our study suggest that trace elements and PAHs, especially when the monitored area presents a significant frequency of high-speed winds, can have a different diagnostic application depending on the spatial scale at which the effects of anthropogenic sources are evaluated. Indeed, the former are associated with both coarse and fine-ultrafine particles, i.e. with very different deposition velocities so that their variation at both the local scale (tens-hundreds of metres from the source) and the whole study area scale (kilometres from the source) can be used to evaluate the environmental impact of the selected sources. Although the PAHs with the highest representation in exhaust emissions, i.e. volatile and semivolatile PAHs, may have a relatively variable gas/particulate phase partition, the particles they are associated with have nanometric size, i.e. with quite low deposition velocities. This means that their spatial variation might be more effectively used to trace the role of an anthropogenic source when evaluated at the whole study area scale. Such a result can be made possible especially when testing quantitative relationships between winds and the spatial variation of the selected substances. Because the calculation of the parameter PNTWRS is independent of the type of biomonitor selected, it can be used with whatever kind of organism shows a bioaccumulation correlating in a statistically significant way with the exposure to atmospheric contaminants. Our results suggest that this parameter can be successfully applied when dealing with different anthropogenic sources of pollutants as it is not affected by the height of emission or the characteristics of fuels and combustion processes. Attention should be paid to the topography of the study area. Indeed, the higher the roughness of the territory the weaker could be the association with the spatial variation of contaminants due to the generation of eddies which, locally, increase deposition phenomena. An evaluation of the coefficient of variation between iso-altitudinal lines is suggested.

At the local scale (mainly the LTO pathways), Lamezia Terme Airport proved to be a source of trace elements such as Zn, Mo, Cu, Co, Mn, Ni, V and Al but not of volatile and semivolatile PAHs. The PIT zone was found to be a square kilometre-scale source of both Mo and Ni (and secondarily V) and total PAHs. This outcome was probably due to the much longer-lasting activities that generate these substances (APU and GSE engine operations, aircraft taxiing) compared to those of the LTO pathways. From a management point of view, we consider this a remarkable result. Indeed, the central role of the PIT zone of an airport in promoting environmental contamination could be mitigated by both the use of less polluting GSEs and systematic avoidance of the unnecessary reactivation of APUs long before the effective take-off time. Lamezia Terme Airport benefits from strong winds that lessen the potential role of its PIT zone as a contaminants source, but airports located in less favourable climate zones could have a much greater effect on the air quality of the surrounding territory. Road traffic was a source, at the local scale only, of some trace elements, i.e. Cu, Sb and Mo, but not of PAHs. The highest levels of traffic rate recorded in the north/north-east part of the study area provided the main extra-airport contribution to the spatial variation of Mo, Ni, V (because of the similar applications in anti-wear technologies) and total PAHs within a range of square kilometres.

## CRediT authorship contribution statement

**L. Lucadamo:** Conceptualization, Supervision, Formal analysis, Writing - original draft. **L. Gallo:** Supervision, Writing - original draft, Project administration. **G. Vespasiano:** Formal analysis, Visualization. **A. Corapi:** Writing - review & editing, Investigation, Data curation, Formal analysis.

## Declaration of Competing Interest

The authors declare that they have no known competing financial interests or personal relationships that could have appeared to influence the work reported in this paper.

## Appendix A. Supplementary data

Supplementary data to this article can be found online at https://doi.org/10.1016/j.ecolind.2021.107474.

## References


Abegglen, M., 2016. Physical and Chemical Characterization of Non-Volatile Aircraft Engine Exhaust. A dissertation submitted to ETH Zurich for the degree of Doctor of Sciences. http://www.vups.ch/Verein/Themen/PhD_Dissertation-Manuel_Abegglen.pdf (accessed 10 January 2020).

ACI, 2016. Parco Veicolare in Italia. http://www.comuni-italiani.it/079statistiche.html (accessed 15 December 2019).

Agrawal, H., Sawant, A.A., Jansen, K., Miller, J.W., Cocker III, D.R., 2008. Characterization of chemical and particulate emissions from aircraft engines. Atmos. Environ. 42 (18), 4380–4392. https://doi.org/10.1016/j.atmosenv.2008.01.069.

Air Quality Expert Group, 2012. Fine Particulate Matter (PM2.5) in the United Kingdom. Report from the Air Quality Expert Group to the Department of the Environment, Food and Rural Affairs, Scottish Government, Welsh Government, and Department of the Environment in Northern Ireland, on fine Particulate Matter (PM2.5) in the United Kingdom. https://assets.publishing.service.gov.uk/government/uploads/system/uploads/attachment_data/file/69635/pb13837/aqeg-fine-particle-matter-20121220.pdf (accessed 10 December 2019).

Amato, F., Moreno, T., Pandolfi, M., Querol, X., Alastuey, A., Delgado, A., Pedrero, M., Cots, N., 2010. Concentrations, sources and geochemistry of airborne particulate matter at a major European airport. J. Environ. Monitor. 12 (4), 854–862. https://doi.org/10.1039/b925439k.

Anu, N., Rangabhashiyam, S., Antony, R., Selvaraju, N., 2015. Optimization of wind speed on dispersion of pollutants using coupled receptor and dispersion model. Sadhana 40 (5), 1657–1666. https://doi.org/10.1007/s12046-015-0396-0.

AZO Materials, 2009. Carbon Filter Analysis by Atomic Emission Spectroscopy (CFA/AES). Detecting Large Wear Particles in Fluids. https://www.azom.com/article.aspx?ArticleID=4578 (accessed 15 January 2020).

Benner, B.A., Gordon, G.E., Wise, S.A., 1989. Mobile sources of atmospheric polycyclic aromatic-hydrocarbons - a roadway tunnel study. Environ. Sci. Technol. 23, 1269–1278. https://doi.org/10.1021/es00068a014.

Bennett, M., Christie, S.M., Graham, A., Thomas, B.S., Vishnyakov, V., Morris, K., Peters, D.M., Jones, R., Ansell, C., 2011. Composition of smoke generated by landing aircraft. Environ. Sci. Tech. 45 (8), 3533–3538. https://doi.org/10.1021/es1027585.

Blasco, M., Domeno, C., Nerin, C., 2008. Lichens biomonitoring as feasible methodology to assess air pollution in natural ecosystems: combined study of quantitative PAHs analyses and lichen biodiversity in the Pyrenees Mountains. Anal. Biochem. Chem. 391 (3), 759–771. https://doi.org/10.1007/s00216-008-1890-6.

Bostrom, C.E., Gerde, P., Hanberg, A., Jernstrom, B., Jahansson, C., Kyrklund, T., Rannug, A., Tornqvist, M., Victorin, K., Westerholm, R., 2002. Cancer risk assessment, indicators, and guidelines for polycyclic aromatic hydrocarbons in the ambient air. Environ. Health Persp. 100 (3), 451–488. https://doi.org/10.1289/ehp.110-1241197.

Boyle, K.A., 1996. Evaluating particulate emissions from jet engines: Analysis of chemical and physical characteristics and potential impacts on coastal environments and human health. Transport. Res. Re.: J. Transp. Res. Board 1517 (1), 1–9 https://doi.org/10.3141%2F1517-01.

Brusseau, M.L., 2006. Physical processes affecting contaminant, transport and fate, in: Pepper, I.L., Gerba, C.P., Brussaux, M.L. (Eds.), Environmental and Pollution Science. Elsevier, London, pp. 79-104.

Choi, W., Hu, S., He, M., Kozawa, K., Mara, S., Winer, A.M., Paulson, S.E., 2013. Neighbourhood-scale air quality impacts on emissions from motor vehicles and aircraft. Atmos. Environ. 80, 310–321. https://doi.org/10.1016/j.atmosenv.2013.07.043.

D'Agosto, M.A., Ribeiro, S.K., 2003. Airport Contributions to Local Air Pollution Case Study: Rio de Janeiro International Airport. Transactions on Ecology and the Environment, vol. 66, WIT Press, ISSN 1743-3541. https://www.witpress.com/Secure/elibrary/papers/AIR03/AIR03043FU.pdf (accessed 12 January 2020).

Danish EcoCouncil, 2019. Air Pollution in Airports. ISBN 978-87-92044-37-2. http://www.projectcleanair.eu/measurements/documents/Air%20pollution%20in%20airports.pdf (accessed 16 September 2019).

Dongarrà, G., Manno, E., Varrica, D., 2009. Possible markers of traffic-related emissions. Environ. Monit. Assess. 154 (1–4), 117–125. https://doi.org/10.1007/s10661-008-0382-7.

EASA, 2013. ICAO Aircraft Engine Emissions Databank. European Aviation Safety Agency. https://www.easa.europa.eu/easa-and-you/environment/icao-aircraft-engine-emissions-databank (accessed 19 October 2019).

ENAC, 2017. Dati di Traffico 2017. https://www.enac.gov.it/pubblicazioni/dati-di-traffico-2017 (accessed 24 September 2019).

ENAC-ASSAEROPORTI, 2019. Principali caratteristiche tecniche degli aeroporti italiani certificati ENAC. www.mit.gov.it/mit/mop_all.php?p_id=23452 (accessed 18 September 2019).

ESDAC, 2020. European Soil Data Centre. Carta dei suoli d'Italia. Last update, September 2020. https://esdac.jrc.ec.europa.eu/images/Eudasm/IT/2012CartaSuoliItalia.jpg (accessed 10 September 2020).

EURL-SRM, 2013. Analysis of Organotin-Pesticides by the QUuEChERS Method-Impact of acidifying on the recoveries. EU Reference Laboratory for Pesticides Requiring Single Residue Methods. CVUA Stuttgart, Schaflandstr. 3/2, 70736 Fellbach, Germany. www.eurl-pesticides.eu/library/docs/srm/Eurl_observations_Organotins.pdf (accessed 18 September 2020).

FAA, 2015. Aviation emissions, Impacts & Mitigation: A Primer. Office of Environment and Energy. Federal Aviation Administration. https://www.faa.gov/regulations_policies/policy_guidance/envir_policy/media/primer_jan2015.pdf (accessed 10 January 2020).

Fang, G.C., Cheng, M.T., Chang, C.N., 1997. Monitoring and modelling the mass, heavy metals and ion species dry deposition in Central Taiwan. J. Environ. Sci. Health A 32 (8), 2183–2199. https://doi.org/10.1080/10934529709376676.

Fleuti, E., Hofmann, P., 2005. Ground Power Unit (GPU) exhaust emissions at Zurich Airport. Unique Flughafen Zurich AG, pp. 18. https://www.zurich-airport.com/~/media/flughafenzh/dokumente/das_unternehmen/laerm_politik_und_umwelt/luft/2005_zrh_apu-emiscalcmeth.pdf (accessed 20 October 2019).

Gunatilake, H., Ganesan, K., Bacani, E., 2014. Evaluation of health impacts of air pollution from power plants in Asia: a practical guide. ADB South Asia Working Paper Series N. 30. ISSN 2313-5867. adb.org/sites/default/files/publication/149583/souh-asia-wp-30.pdf (accessed 18 December 2019).

Hall, D.E., Goodfellow, C.L., Guttmann, H.J., Hevesi, J., McArragher, J.S., Mercogliano, R., Merino, M.P., Morgan, T.D.B., Nancekievill, G., Rantanen, L., Rickeard, D.J., Terna, D., Zemroch, P.J., Heinze, P., 1998a. A study of the number, size & mass of exhaust particles emitted from European vehicles under steady-state and European driving cycle conditions. Report no. 98/51. Prepared for the CONCAWE Automotive Emissions Management Group by its Special Task Force AE/STF-10. Brussels. https://www.concawe.eu/wp-content/uploads/2017/01/rpt_98-51-2003-01972-01-e.pdf (accessed 12 September 2019).

Hall, D.E., Doel, R., Jorgensen, R., King, D.J., Mann, N., Scorletti, P., Heinze, P., 1998b. Polycyclic aromatic hydrocarbons in automotive exhaust emissions and fuels. Report no. 98/55. Prepared for the CONCAWE Automotive Emissions Management Group by its Special Task Force AE/STF-12. Brussels. https://www.concawe.eu/wp-content/uploads/2017/01/rpt_98-55-2004-01306-01-e.pdf (accessed 21 December 2019).

Guidotti, M., Stella, D., Dominici, C., Blasi, G., Owczarek, M., Vitali, M., Protano, C., 2009. Monitoring of traffic-related pollution in a province of central Italy with transplanted lichen Pseudevernia furfuracea. Bull. Environ. Contam. Tox. 83 (6), 852–858. https://doi.org/10.1007/s00128-009-9792-7.

Ho, K.F., Ho, S.S.H., Lee, S.C., Cheng, Y., Chow, J.C., Watson, J.G., Louie, P.K.K., Tian, L., 2009. Emissions of gas- and particle-phase polycyclic aromatic hydrocarbons (PAHs) in the ShingMun Tunnel, Hong Kong. Atmos. Environ. 43, 6343–6635. https://doi.org/10.1016/j.atmosenv.2009.09.025.

Huttunen-Saarivirta, E., Kuokkala, V.T., Kokkonen, J., Paajanen, H., 2011. Corrosion effects of runway de-icing chemicals on aircraft alloys and coatings. Mater. Chem. Phys. 126, 138–151. https://doi.org/10.1016/j.matchemphys.2010.11.049.

Iijima, A., Sato, K., Yano, K., Tago, H., Kato, M., Kimira, H., Furuta, N., 2007. Particle size and composition distribution analysis of automotive brake abrasion dusts for the evaluation of antimony sources of airborne particulate matter. Atmos. Environ. 41 (23), 4908–4919. https://doi.org/10.1016/j.atmosenv.2007.02.005.

Johansson, C., Norman, M., Burman, L., 2008. Road traffic for heavy metals. Atmos. Environ. 43 (31), 4681–4688. https://doi.org/10.1016/j.atmosenv.2008.10.024.

Kenney, M., Fowler, C., Ratte M., Sanford, P., Pringle, P., Sequeira, C., Didyk, N., 2015. GSE Emissions Inventories. Improving Ground Support Equipment Operational Data for Airport Emissions Modelling. Research Sponsored by the Federal Aviation Administration – Transportation Research Board, Washington D.C. https://www.faa.gov/regulations_policies/policy_guidance/envir_policy/airquality_handbook/media/Air_Quality_Handbook_Appendices.pdf (accessed 18 December 2019).

Keyte, I.J., Albinet, A., Harrison, R.M., 2016. On-road traffic emissions of polycyclic aromatic hydrocarbons and their oxy- and nitro- derivative compounds measured in road. Sci. Total Environ. 566–567, 1131–1142. https://doi.org/10.1016/j.scitotenv.2016.05.152.

Kim, K.H., Lee, S.-B., Woo, D., Bae, G.-N., 2015. Influence of wind direction and speed on the transport of particle bound PAHs in a roadway environment. Atmos. Pollut. Res. 6 (6), 1024–1034. https://doi.org/10.1016/j.apr.2015.05.007.

Kracke, A., 2010. Superalloys, the most successful alloy system of the modern tomes – past, present and future, in: Ott, E.A., Groh, J.R., Banik, A., Dempster, I., Gab, T.P., Helmink, R., Liu, X., Mitchell, A., Sjoberg, G.P., Wusatowska-Sarned, A.(Eds.), 7th International Symposium on Superalloy 718 and Derivatives. TMS (The Minerals, Metals & Materials Society), pp. 13-50. https://www.tms.org/superalloys/10.7449/2010/Superalloys_2010_13_50.pdf (accessed 10 October 2019).

Kuhlman, M.R., Chuang, J.C., 1989. Characterization of chemicals on engine exhaust particles: F101 and F110 engines. Battelle Memorial Institute, 505 King Avenue, Columbus OH 43201-2693 Final Report ESL-TR-89-20. https://apps.dtic.mil/dtic/tr/fulltext/u2/a242883.pdf (accessed 20 December 2019).

Kinsey, J.S., Timko, M.T., Herndon, S.C., Wood, E.C., Yu, Z., Miake-Lye, R.C., Lobo, P., Whitefield, P., Hagen, D., Wey, C., Anderson, B.E., Beyerdorsf, A.J., Hudgins, C.H., Thornhill, K.L., Winstead, E., Howard, R., Bulzan, D.I., Tacina, K.B., Knighton, W.B., 2012. Determination of the emissions from an aircraft auxiliary power unit (APU) during the Alternative Aviation Fuel Experiment (AAFEX). J. Air Waste Manag. Ass. 62 (4), 420–430. https://doi.org/10.1080/10473289.2012.655884.

Liu, H., Fang, C., Zhang, X., Wang, Z., Bao, C., Li, F., 2017. The effect of natural and anthropogenic factors on haze pollution in Chinese cities: a spatial econometrics approach. J. Clean. Prod. 165, 323–333. https://doi.org/10.1016/j.jclepro.2017.07.127.

Lucadamo, L., Corapi, A., Gallo, L., 2017. Local wind monitoring matched with lichen Pseudevernia furfuracea (L.) Zopf transplantation technique to assess the environmental impact of a biomass power plant. Turk. J. Bot. 41, 145–160. https://doi.org/10.1016/j.apr.2017.03.002.

Lucadamo, L., Corapi, A., Gallo, L., 2018. Evaluation of glyphosate drift and anthropogenic atmospheric trace elements contamination by means of lichen transplants in a southern Italian agricultural district. Air Qual. Atmos. Health 11 (3), 325–339. https://doi.org/10.1007/s11869-018-0547-7.

Lucadamo, L., Corapi, A., Loppi, S., De Rosa, R., Barca, D., Vespasiano, G., Gallo, L., 2016. Spatial variation in the accumulation of elements in thalli of the lichen Pseudevernia furfuracea (L.) Zopf Transplanted around a biomass power plant in Italy. Arch. Environ. Contam. Tox. 70 (3), 506–521. https://doi.org/10.1007/s00244-015-0238-4.

Lv, B., Cai, J., Xu, B., Bai, Y., 2017. Understanding the Rising Phase of PM2,5 concentration evolution in large china cities. Sci. Rep. 7, 46456. https://doi.org/10.1038/srep46456.

Masiol, M., Harrison, R.M., 2014. Aircraft engine exhaust emissions and other airport-related contributions to ambient air pollution: a review. Atmos. Environ. 95, 409–455. https://doi.org/10.1016/j.atmosenv.2014.05.070.

Massas, I., Ioannou, D., Kalivas, D., Gasparatos, D., 2016. Distribution of heavy metals concentrations in soils around the international Athens airport (Greece), an assessment on preliminary data. B. Geol. Soc. Greece 50 (4), 2231–2240. https://doi.org/10.12681/bgsg.14279.

Miri, M., Ehrampoush, M.H., Ghaffari, H.R., Ebrahimi, H., Rezai, A.M., Najafpour, F., Fathabadi, Z.A., Aval, M.Y., Ebrahimi, A., 2017. Atmospheric heavy metals biomonitoring using a local Pinus eldarica tree. Health Scope 6 (1). https://doi.org/10.17795/jhealthscope-39241.

Mohan, S.M., 2016. An overview of particulate dry deposition: measuring methods, deposition velocity and controlling factors. Int. J. Environ. Sci. Tehnol. 13 (1), 387–402. https://doi.org/10.1007/s13762-015-0898-7.

Nunes, L.M., Stigter, T.Y., Teixeira, M.R., 2011. Environmental impacts on soil and groundwater at airports: origin, contaminants of concern and environmental risks. J. Environ. Monit. 13 (11), 3026–3039. https://doi.org/10.1039/c1em10458f.

Padhra, A., 2018. Emissions from auxiliary power units and ground power units during intraday aircrafts turnarounds at European airports. Transport Res. Part D 63, 433–444. https://doi.org/10.1016/j.trd.2018.06.015.

Pant, P., Harrison, R.M., 2013. Estimation of the contribution of road traffic emissions toparticulate matter concentration from field measurements: a Review. Atmos. Environ. 77, 78–97. https://doi.org/10.1016/j.atmosenv.2013.04.028.

Press-Kristensen, K., 2012. Air Pollution in Airports. Ultrafine particles, solutions and successful cooperation. Published by The Danish EcoCouncil. ISBN 978-87-92044-37-2. www.project-cleanair.eu/measurements/documents/Air%20Pollution%20in%20airports.pdf (accessed 18 December 2019).

Riga-Karandinos, A.N., Karandinos, M.G., 1998. Assessment of air pollution from a lignite power plant in the plain of Megalopolis (Greece) using as biomonitors three species of lichens: impacts on some biochemical parameters of lichens. Sci. Total Environ. 215 (1–2), 167–183. https://doi.org/10.1016/S0048-9697(98)00119-3.

Rogers, F., Arnott, P., Zielinska, B., Sagebiel, J., Kelly, K.E., Wagner, D., Lighthy, J.S., Sarofim, A.F., 2005. Real-time measurements of jet aircraft engine exhaust. J. Air Waste Manage. 55 (5), 583–593. https://doi.org/10.1080/10473289.2005.10464651.

SACAL, 2015. Aeroporto di Lamezia terme: Piano quadriennale degli investimenti 2016-2019. http://www.assaereo.it/documenti/sacal/documenti%20consultazione%20luglio20%2016/piano_quadriennale_2016-2019_Lamezia.pdf (accessed 18 July 2019).

Sarvi, A., Lyyranen, J., Jokiniemi, J., Zevenhoven, R., 2011. Particulate emissions from large-scale medium speed diesel engines: 2 chemical composition. Fuel Process. Technol. 89 (5), 520–527. https://doi.org/10.1016/j.fuproc.2011.06.021.

Schlenker, W., Walker, W.R., 2016. Airports, air pollution, and contemporaneous health. Rev. Econ. Stud. 83 (2), 768–809. https://doi.org/10.1093/restud/rdv043.

Sehmel, G.A., Hodgson, W.H., 1978. A model for predicting dry deposition of particles and gases to environmental surface, DOEreport PNLSA-6721. Pacific Northwest Laboratory, Richland, WA. https://www.osti.gov/biblio/6717982 (accessed 18 December 2019).

Serelis, K.G., Kafkala, I.G., Parpodis, K., Lazaris, S., 2010. Anthropogenic and geogenic contamination due to heavy metals in the vast area of Vari, Attica. Bulletin of the Geological Society of Greece, Proceedings of the 12th International Congress. Patras, May 2010, XLIII(5):2390–2397. https://doi.org/10.12681/bgsg.11639.

Songy, A., Vallet, J., Gantet, M., Boos, A., Ronot, P., Tarnus, C., Clement, C., Larignon, P., Goddard, M.L., Fontaine, F., 2019. Sodium arsenite effect on Vitis vitifera L. J. Plant Physiol. 238, 72–79. https://doi.org/10.1016/j.jplph.2019.05.010.

Spicer, W.C., Holdren, M.C., Smith, D.L., Hughes, D.P:, Smith, M.D., 1990. Chemical Composition of Exhaust from Aircraft Turbine Engines. The American Society of Mechanical Engineers, 90-GT-34 presented at the Gas and Aeroengine Congress and Exposition, June 11-14, 1990 Brussels, Belgium. http://citeseerx.ist.psu.edu/viewdoc/download?doi=10.1.1.911.4790&rep=rep1&type=pdf (accessed 21 October 2019).

Szewczynska, M., Dabrowska, J., Pyrzynska, K., 2017. Polycyclic aromatic hydrocarbons in the particles emitted from the diesel and gasoline engines. Pol. J. Environ. Stud. 26 (2), 801–807. https://doi.org/10.15244/pjoes/64914.

TRANSPHORM, 2014. Transport related Air Pollution and Health impacts – Integrated Methodologies for Assessing Particulate Matter. University of Hertfordshire Higher Education Corporation U.K.. Project funded by European Commission – FP7-Environment. ID : 243406. www.cordis.europa.eu/project/id/243406 (accessed 20 September 2020).

Usmani, A.M., Donley, M., 2002. Aircraft-coating, weathering studies by analytical methods. J. Appl. Polym. Sci. 86 (2), 294–313. https://doi.org/10.1002/app.10960.

Vieira de Souza, C., Correa, S.M., 2016. Polycyclic aromatic hydrocarbons in diesel emission, diesel fuel and lubricant oil. Fuel 165, 925–931 https://doi.org/10.1016%2Fj.fuel.2016.08.054.

Vukovic, G., Urosevic, M.A., Skrivani, S., Verge, K., Tomasevic, M., Popovic, A., 2017. The first survey of airborne trace elements at airport using moss bag technique. Environ. Sci. Pollut. Res. 24 (17), 15107–15115. https://doi.org/10.1007/s11356-017-9140-0.

Waeber, M., Aust, S., Johannsen, K., Pompe, F., Heimberg, J., 2015. Biomonitoring with curly kale and grass exposure in the vicinity of Berlin Brandenburg Airport - Long-term investigation of the possible environmental impact of air traffic and airport operations. Gefahrst. Reinhalt. Luft. 75 (4), 137–142.

Wang, J.L., Xie, X., Fang, C., 2019. Temporal and spatial distribution characteristics of atmospheric particulate matter (PM10 and PM 2.5) in changchun and analysis of its influencing factors. Atmosphere 10 (11), 651. https://doi.org/10.3390/atmos10110651.

Wood, E., Herndon, S., Miake-Lye, R., Nelson, D., Seeley, M., 2008. Aircraft and Airport-Related Hazardous Air Pollutants: Research Needs and Analysis. Airport Cooperative Research Programme, Report 7. Transportation Research Board of the National Academies. ISSN 1935-9802. www.trb.org/Publications/Blurbs/160113.aspx (accessed 19 December 2020).

Xue, J., Li, Y., Wang, X., Durbin, T.D., Johnson, K.C., Karavalakis, G., Asa-Awuku, A., Villela, M., Quiros, D., Hu, S., Huai, T., Ayala, A., Jung, H.S., 2015. Comparison of vehicle exhaust particle size distributions measured by SMPS and EEPS during steady-state conditions. Aerosol Sci. Tech. 49 (10), 984–996. https://doi.org/10.1080/02786826.2015.1088146.

Zhan, D., Kwan, M.-P., Zhang, W., Yu, X., Meng, B., Liu, Q., 2018. The driving factors of air quality in China. J. Clean. Product. 197, 1342–1351. https://doi.org/10.1016/j.jclepro.2018.06.108.

Zhang, Y., Wang, Q., 2017. Methods for determining unimpeded aircraft taxiing time and evaluating airport taxiing performance. Chin. J. Aeronaut. 30 (2), 523–537. https://doi.org/10.1016/j.cja.2017.01.002.

Zhou, Y., Levy, J.I., 2009. Between-airport heterogeneity in air toxics emissions associated with individual cancer risk thresholds and population risks. Environ. Health 8, 8–12. https://doi.org/10.1186/1476-069X-8-22.

Zielinska, B., Sagebiel, J., Arnott, W.P., Rogers, C.F., Wagner, D.A., Lighty, J.S., Sarofim, A.F., Palmer, G., 2004. Phase and size distribution of polycyclic aromatic hydrocarbons in diesel and gasoline vehicle emissions. Environ. Sci. Technol. 38 (9), 2557–2567. https://doi.org/10.1021/es030518d.